GCM evaluation of a mechanism for El Niño triggering by the El Chichón ash cloud

Alan Robock
Department of Meteorology, University of Maryland, College Park

Karl E. Taylor
Lawrence Livermore National Laboratory, Livermore, California

Georgiy L. Stenchikov and Yuhe Liu[1]
Department of Meteorology, University of Maryland, College Park

Abstract. The El Chichón volcanic eruption in 1982 was immediately followed by the strongest El Niño of the century in 1982-83. We investigate a possible mechanism proposed by Hirono whereby volcanic eruptions might trigger or enhance El Niños. Three distributions of volcanic ash aerosol in the troposphere over the eastern Pacific Ocean were used to force simulations with a modified version of the NCAR CCM1 atmospheric general circulation model for the month of April 1982, using observed sea surface temperatures. Only in the case of mid-tropospheric heating is there a strong dynamical reaction in the atmosphere resulting in a weakening of the trade winds in the eastern Pacific Ocean north of the equator, consistent with surface wind observations and with the first part of Hirono's theory. However, the 1982 ENSO event had started before this wind anomaly, and only trade wind collapses in the western equatorial Pacific can initiate El Niños. The results suggest that, while tropospheric aerosols from volcanic eruptions can influence atmospheric circulation, the timing and location of the El Chichón eruption and the large ENSO event that followed was a coincidence, and that Hirono's mechanism was not responsible for the strength or timing of the El Niño.

On March 29 and April 4, 1982, the El Chichón volcano in southern Mexico erupted, injecting massive amounts of aerosols into the troposphere and stratosphere, with the April 4 eruption being one of the largest of the century [*Robock*, 1983]. Satellite images of the eruption [*Robock and Matson*, 1983] showed that aerosol clouds were advected both eastward and westward by winds at different levels in the atmosphere. The largest cloud, from the April 4 eruption, went westward, circling the globe in 3 weeks in the stratosphere. At the same time, visible satellite imagery revealed a cloud of aerosols over the eastern Pacific Ocean which remained there for the entire 3 week period [see Figs. 1-2 of *Robock and Matson*, 1983] and perhaps longer. The optical depth of this cloud was estimated to be approximately 0.5 at the center during the periods April 5-10 and 20-25 [*Durkee et al.*, 1991]. Using all available information, including the synoptic situation at the time, we conclude that this cloud consisted of large ash particles in the troposphere that were gradually settling out of the stratospheric cloud due to their larger size and fall speed. The dry weather conditions, preventing wet removal, and the weak horizontal winds which varied in direction at different levels, allowed them to remain in essentially the same location for several weeks [*Hirono*, 1988].

Beginning in April 1982, as indicated by the Southern Oscillation Index, an unpredicted and unprecedented El Niño began, resulting in the largest warm ENSO (El Niño/Southern Oscillation) event of the century, with record warm temperatures in the eastern equatorial Pacific Ocean and remote temperature and precipitation anomalies in distant locations [*Halpert and Ropelewski*, 1992]. Due to the coincidence of the beginning of the ENSO event and the El Chichón eruption, several suggestions were made as to a cause and effect relationship [*Schatten et al.*, 1984; *Strong*, 1986], even going so far as to erroneously suggest that most El Niños were caused by volcanic eruptions [*Handler*, 1986].

Hirono [1988] proposed the only plausible theory, in our opinion. His theory had two parts: 1) tropospheric aerosols from the El Chichón eruption induced an atmospheric dynamical response producing a trade wind collapse, and 2) the trade wind reduction produced an oceanographic response which affected the timing and strength of the resulting El Niño. Even if part 1 is valid, the location and timing of the trade wind changes determine whether part 2 is valid. Hirono used a linear steady state atmospheric model [*Gill*, 1980] to calculate tropospheric wind anomalies due to the presence of tropospheric volcanic aerosols. He considered two tropospheric aerosol distributions. One was a zonally uniform upper tropospheric aerosol cloud, which *Graf et al.* [1992] have already shown would not produce the necessary tropospheric circulation to initiate an El Niño. The other distribution was in the region of the satellite-observed aerosols in the eastern Pacific Ocean. The heating induced in the troposphere by the volcanic aerosols produced an anomalous cyclonic circulation resulting in westerly anomalies in the trade winds near the surface, but his idealized experiments were not specific about the location of this change in the trade winds. He concluded that the slackening of the trade winds would be enough to trigger the ENSO event [*Hirono*, 1988], citing the results of *Cane and Zebiak* [1985]. This theory has not been generally accepted, due to the simple nature of the heating profiles and

[1]now at Center for Analysis and Prediction of Storms, University of Oklahoma, Norman

Copyright 1995 by the American Geophysical Union.

Paper number 95GL02065
0094-8534/95/95GL-02065$03.00

model used, and the progress of modeling El Niños without volcanic eruptions, including the recent 1991 event which began just *before* the Pinatubo volcanic eruption in June 1991 in the Philippines. Hirono's theory, however, does not suggest that all eruptions enhance or trigger warm ENSO events. It is specific to the El Chichón eruption, as it depends on the *longitude* of the *tropospheric* aerosols.

Therefore, we decided to test Hirono's theory by using an atmospheric general circulation model (GCM) which would allow us to test different vertical distributions of aerosols, allow for non-linear reactions to the imposed aerosol forcing, including cloud radiative and thermodynamic feedbacks, and determine the location and amplitude of trade wind changes, if any. We used the National Center for Atmospheric Research Community Climate Model 1 [*Williamson et al.*, 1987], modified at Lawrence Livermore National Laboratory to calculate the solar radiative effects of aerosols within the model radiation code [*Taylor and Ghan*, 1992]. We used an R15 spectral resolution corresponding to a grid spacing of 4.5° in latitude by 7.5° in longitude, and 12 vertical levels. The model includes interactive convective and layer clouds, but does not include aerosol transport, removal, longwave effects, or indirect effects on clouds, and we imposed a constant aerosol distribution during the 1-month runs. Using observed monthly-average sea surface temperatures (SSTs), we ran the model starting from November 1, 1981, through the end of April 1982, twice, with two different sets of initial conditions, in order to produce two statistically-independent control simulations. The initial conditions were taken from two different Novembers of a multiyear simulation with this model, but the particular initial values are irrelevant since they are essentially "forgotten" long before the next April.

As input to our GCM, we had to prescribe the optical characteristics and vertical profile of the volcanic aerosols. Initial experiments (not shown here) with stratospheric sulfate aerosols produced no response that would affect ENSO during the 8 months following the eruption, in agreement with previous GCM results [*Robock and Liu*, 1994]. We therefore decided to concentrate on tropospheric aerosols during the first month after the eruption. For at least 2 weeks the stratospheric aerosol cloud sped around the earth leaving the tropospheric aerosols uncovered in the eastern Pacific [*Robock and Matson*, 1983]. There were no direct measurements of this aerosol cloud in the eastern Pacific, so we had to make reasonable choices of the horizontal extent and total optical depth of about 0.5 that were consistent with the existing satellite measurements. Volcanic sulfate aerosols take several weeks or months to form and are purely reflecting in the ultraviolet and visible bands, and therefore, with this optical depth, even taking into account infrared absorption, would have been unable to produce immediate significant heating or local dynamical reactions. For the first two months, significant amounts of ash particles were observed in the El Chichón cloud. *Gooding et al.* [1983] estimated an initial stratospheric injection of more than 480 tons of ash, which was much more absorbing than sulfate aerosol, with a single-scattering albedo of 0.9 or less [*Deepak and Gerber*, 1983]. The ash particles have a different chemical structure and larger size (submicron to as large as 40 μm) than sulfate aerosols. *Woods and Chuan* [1983] found that 60-80 % of the aerosol mass measured in April was ash particles between 3 and 20 μm. For these reasons, we assumed that the aerosol cloud in the troposphere was dominated by ash particles.

Preliminary numerical experiments with the GCM showed a very high sensitivity of the atmospheric dynamical reaction to the aerosol-induced heating rates and their vertical distribution. Hirono in his calculations used only the first term of a Fourier expansion in the vertical, so the prescribed heating rates in his analytical model were proportional to the cosine of the altitude, vanishing at the top and the bottom of troposphere, and reaching a maximum value of 2 K day^{-1} in the middle troposphere. Aerosols would have a time-dependent distribution that would not be this smooth. Because there are no observations of the aerosol vertical structure, we used physical arguments to develop 3 profiles with the same total optical depth as observed [*Durkee et al.*, 1991].

The fall speed w of the aerosol particles depends on particle radius and density, and decreases in denser atmospheric layers [*Oberbeck et al.*, 1983]. The decrease of fall speed with depth in the atmosphere leads to a concentration of aerosols in the lower layers of the troposphere above the boundary layer, where turbulence and moist processes remove the aerosol particles. For the period of interest, the mixing ratio of the falling aerosol particles of a given size will have a maximum at some layer in the troposphere, a sharp cutoff below this layer, and will decrease above this level with altitude. Therefore, we constructed three aerosol profiles for the GCM calculations, one with the aerosols concentrated in the upper troposphere (profile a), one with them in the mid-troposphere (profile b), and one in the lower troposphere (profile c). The maximum heating rate for each profile was about 1.5 K day^{-1}.

Our suite of experiments included a control case (without volcanic aerosols) and 3 perturbation cases (one for each of the aerosol profiles described above). We began each of the perturbed simulations on April 1, 1982, by imposing one of the 3 different vertical distributions of aerosols in the troposphere in the region of the eastern Pacific Ocean from 0-30°N and 60-150°W, corresponding to the location of the El Chichón aerosol cloud from satellite observations. To allow the atmosphere to react strongly enough to overcome the natural weather variability, we ran the model for 30 days with constant aerosol forcing and show results averaged for the last 8 days of the run. An alternative, more expensive strategy, would have been to conduct many more shorter runs and average over a period closer to the aerosol input. Our 30-day runs should provide an upper limit on the expected response for each aerosol profile, because in nature the aerosol cloud would tend to disperse.

By using observed SSTs for both the control and aerosol experiments, we prevent circulation changes that might result from any reduction in SSTs caused by the volcanic aerosol. The reduction in surface radiation for the region of the aerosols averages approximately 24 W m^{-2} for profile a and 30 W m^{-2} for profiles b and c and would lead to a reduction of SST of 0.3-0.4 K if imposed continuously for 30 days for a 50-m oceanic mixed layer. Since in our simulations we prescribed actual SSTs, any surface cooling effect has been incorporated into both control and aerosol calculations. If we had accounted for differences in surface temperature of a few tenths of a degree between the control and aerosol experiments, we might have found a slightly weaker atmospheric response to the aerosol, but given that direct atmospheric heating induced atmospheric temperature changes of about 3-6 times this amount in the atmosphere averaged over the region of the aerosols, and 10 times this amount at the center of the aerosol cloud, we do not believe

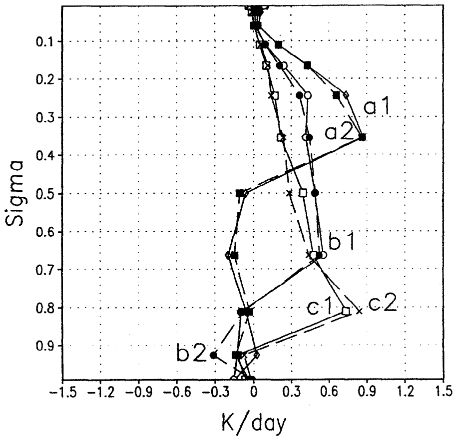

Figure 1. Short wave radiative heating anomaly profiles for 3 different vertical distributions of tropospheric aerosols (experiment *minus* control), averaged over the region 0-30°N and 60-150°W, where the aerosol was located, for the last 8 days of the 30-day GCM simulations for April 1982, described in the text. For each of the 3 aerosol distributions (a, b, and c) the numbers 1 and 2 distinguish between the 2 cases with different initial conditions. The heating rates at the center of this region would be larger than this average and correspond to the 1.5 K day^{-1} described in the text.

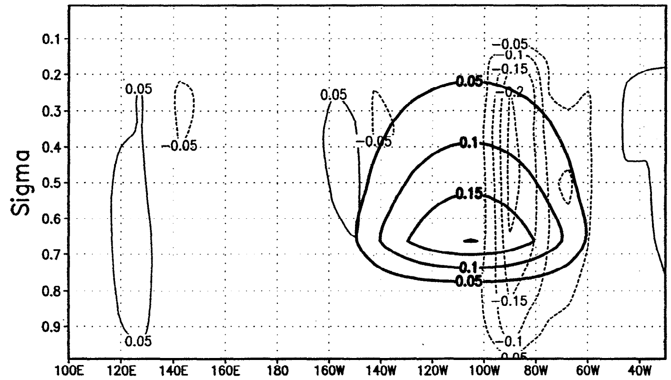

Figure 2. Anomaly results (experiment *minus* control) averaged for the last 8 days of the 2 profile b 30-day runs: vertical motion cross-section from 10-20°N, in units of Pa sec^{-1}. The region of large negative values at 90°W is the upward motion induced by the aerosol heating. The thick dashed contours show the imposed aerosol profile in g m^{-2}.

our neglect of surface temperature changes would have had a major impact on the results.

The resulting shortwave radiative heating profiles, averaged over this region for the 6 runs, are shown in Fig. 1. The different profiles can be thought of as a progression of the cloud downward as it sinks in the atmosphere. The vertical distribution of the aerosol amount is shown in Fig. 2 and the horizontal distribution is shown in Fig. 3a. The aerosol optical properties [*Deepak and Gerber*, 1983] vary from those for sulfate aerosols in the stratosphere to those of ash particles at the bottom of the aerosol layer.

For both experiments with profile b, the resulting dynamical reaction produced upward motion in the region of the aerosols (Fig. 2) and a decrease of the easterly trade winds at the surface (Fig. 3a). Since the normal trade winds are easterly (negative u-component), the increase in u represents a trade wind decrease. This agrees with Hirono's theory as far as the effect on surface winds. Observations of surface winds on the Equator at 95°W and 108°W [M. McPhaden, personal communication, 1995] do not show these reductions but are a bit outside the region shown in Fig. 2. Monthly-average observations of u-component wind anomalies (Figs. 3b-d), however, show a pattern in May 1982 somewhat like the simulated pattern (Fig. 3a) in the region of the aerosols, but of smaller amplitude. Since we show the results for the period April 22-30, and stopped our integration then, the May observations may be the most representative for comparison, but this apparent agreement between simulated and observed wind anomalies might be due to chance alone.

In contrast to profile b, there was no decrease of the trade winds in either of the 2 runs with profiles a and c. This suggests that only at a certain time in the descent of the aerosol cloud was it in the proper position to reduce the trade winds. For both of the profile a runs, a cyclonic circulation developed, as was the case for profile b, but the circulation developed only in the upper part of the troposphere, and a compensating anticyclonic circulation developed beneath it, acting to enhance the trade winds. This did not contradict our previous understanding of the effects of an elevated heat source.

The lack of a response from the profile c experiments was more surprising, as profile c did not differ that much from profile b, so we investigated further. We discovered that for both profiles a and b, the convective heating of the atmosphere (Fig. 4) did not differ significantly for the control and

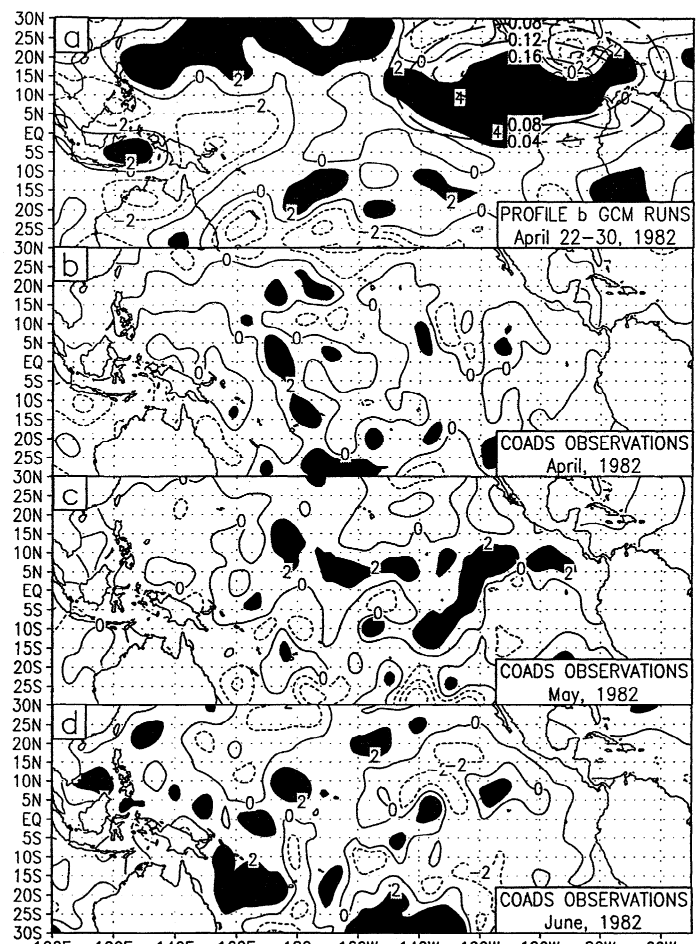

Figure 3. a. Zonal (east-west) wind anomalies (see Fig. 2) at the surface (the lowest model level, 991 mb) in m sec^{-1}. The long dashed contours show the horizontal distribution of the imposed aerosols in g m^{-2} at the level of peak concentration (670 mb). The large positive anomaly under the aerosol cloud is the trade wind reduction. b-d. COADS observed surface zonal wind anomalies for April, May, and June 1982 [*Woodruff et al.*, 1987]. Anomalies > 2 m sec^{-1} are shaded.

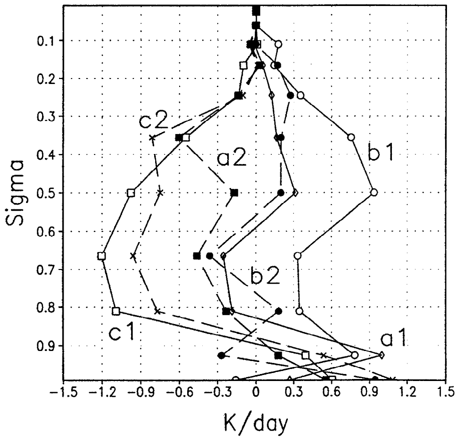

Figure 4. Convective heating anomaly profiles for the same cases as in Fig. 1. Note that for both profile c runs, the suppression of convective heating by the aerosol more than compensates for the direct heating from the aerosol (Fig. 1).

experiment cases, and the anomalous aerosol heating produced an anomalous total heating of the region of the aerosols not that much different from those shown in Fig. 1. For profile c, however, convective heating was reduced so much (Fig. 4) that it more than compensated for the aerosol heating, resulting in no net heating of the column and therefore no dynamical response.

We have demonstrated that tropospheric aerosols from the El Chichón eruption of 1982 could have produced a trade wind reduction in the eastern North Pacific at the end of April and beginning of May 1982, verifying that part of the theory of *Hirono* [1988] and adding detail to the spatial scale of the response. Using a non-linear GCM, we have shown a large sensitivity to the heating profile, showing that aerosols too high or too low in the troposphere would not produce the effect. We have also shown that potential feedback processes in the atmosphere previously not investigated, such as convection, are not strong enough to cancel the aerosol effect for mid-tropospheric heating, and that Hirono's linear theory connecting a heat source in the troposphere to a slackening of the trade winds is not undermined by non-linearities in GCMs.

Current understanding of the mechanisms for initiation of El Niños [e.g., *Chao and Philander*, 1993; *Battisti and Sarachik*, 1995], however, show that it is trade wind collapses in the western Pacific, not the eastern Pacific, that are responsible. L. Goddard [personal communication, 1995] has successfully simulated the initiation and amplitude of the 1982-83 El Niño with a numerical ocean model forced with observed winds, and showed that the oceanic component began long before the El Chichón eruption. D. Gu [personal communication, 1995] has applied trade wind anomalies in the eastern Pacific to an oceanic ENSO model and showed that they had only local effects and did not affect the initiation or amplitude of the resulting El Niño. Therefore, while we have validated Hirono's theory as far as the effect of volcanic aerosols on the trade winds, our results provide no support for the idea that the aerosol cloud from the El Chichón eruption was in a position so as to trigger and enhance the 1982-83 El Niño. This result, combined with the recent finding that there is no ENSO signal in any long-term volcanic indices or in volcanic aerosol records in any ice cores [*Robock and Free*, 1995], allows us to conclude that the coincidence of the 1982 El Chichón eruption and the 1982-83 El Niño, was just that – a coincidence.

Acknowledgments. We thank Ingo Kirchner for a valuable review which clarified and changed our conclusions; M. Hirono, Daifang Gu, Lisa Goddard, Ken Sperber, Mike McPhaden, and Jim O'Brien for valuable discussions; and Daifang Gu for the COADS data used in Figs. 3b-d. Supported by NASA grant NAG-5-1835.

References

Battisti. D. S. and E. S. Sarachik, Understanding and predicting ENSO, in *U.S. National Report to International Union of Geodesy and Geophysics: Contributions in Oceanography*, in press, American Geophysical Union, Washington, DC, 1995.

Cane, M. A. and S. E. Zebiak, A theory for El Niño and the Southern Oscillation, *Science*, *228*, 1085-1087, 1985.

Chao, Y., and S. G. H. Philander, On the structure of the Southern Oscillation, *J. Climate*, *6*, 450-469, 1993.

Deepak, A., and H. E. Gerber (Eds.), *Report of the Experts Meeting on Aerosols and Their Climatic Effects*, *WCP-55*, 101 pp., World Climate Research Programme, Geneva, 1983.

Durkee, P. A., F. Pfeil, E. Frost and R. Shema, Global analysis of aerosol particle characteristics, *Atm. Env.*, *25A*, 2457-2471, 1991.

Gill, A. E., Some simple solutions for heat-induced tropical circulation, *Q. J. Roy. Meteor. Soc.*, *106*, 447-462, 1980.

Gooding, J. L., U. S. Clanton, E. M. Gabel, and J. L. Warden, El Chichón volcanic ash in the stratosphere: particle abundances and size distributions after the 1982 eruption, *Geophys. Res. Lett.*, *10*, 1033-1036, 1983.

Graf, H. F., I. Kirchner, R. Sausen, and S. Schubert, The impact of upper-tropospheric aerosol on global atmospheric circulation, *Ann. Geophys.*, *10*, 698-707, 1992.

Halpert, M. S. and C. F. Ropelewski, Surface temperature patterns associated with the Southern Oscillation, *J. Climate*, *5*, 577-593, 1992.

Handler, P., Possible association between the climatic effects of stratospheric aerosols and sea surface temperatures in the Eastern tropical Pacific Ocean, *J. Climatology*, *6*, 31-41, 1986.

Hirono, M., On the trigger of El Niño Southern Oscillation by the forcing of early El Chichón volcanic aerosols, *J. Geophys. Res.*, *93*, 5365-5384, 1988.

Oberbeck, V. R., E. F. Danielsen, K. G. Snetsinger, and G. V. Ferry, Effect of the eruption of El Chichón on stratospheric aerosol size and composition, *Geophys. Res. Lett.*, *10*, 1021-1024, 1983.

Robock, A., The dust cloud of the century, *Nature*, *301*, 373-374, 1983.

Robock, A. and M. P. Free, Ice cores as an index of global volcanism from 1850 to the present, *J. Geophys. Res.*, *100*, 11,549-11,568, 1995.

Robock, A. and Y. Liu, The volcanic signal in Goddard Institute for Space Studies three-dimensional model simulations, *J. Climate*, *7*, 44-55, 1994.

Robock, A. and M. Matson, Circumglobal transport of the El Chichón volcanic dust cloud, *Science*, *221*, 195-197, 1983.

Schatten, K. H., H. G. Mayr, I. Harris, and H. A Taylor, A zonally symmetric model for volcanic influence upon atmospheric circulation, *Geophys. Res. Lett.*, *11*, 303-306, 1984.

Strong, A. E., The effect of El Chichón on the 82/83 El Niño (abstract), *EOS Trans. AGU*, *67*, 880, 1986.

Taylor, K. E. and S. J. Ghan, An analysis of cloud liquid water feedback and global climate sensitivity in a general circulation model, *J. Climate*, *5*, 907-919, 1992.

Williamson, D. L., J. T. Kiehl, V. Ramanathan, R. E. Dickinson, J. J. Hack, Description of NCAR Community Climate Model (CCM1), *NCAR Tech. Note TN-285+STR*, 112 pp., National Center for Atmospheric Research, Boulder, 1987.

Woodruff, S. D., R. J. Slutz, R. L. Jenne, and P. M. Steurer, A comprehensive ocean-atmosphere data set, *Bull. Amer. Meteorol. Soc.*, *68*, 1239-1250, 1987.

Woods, D. C. and R. L. Chuan, Size-specific composition of aerosols in the El Chichón volcanic cloud, *Geophys. Res. Lett.*, *10*, 1041-1044, 1983.

A. Robock and G. L. Stenchikov, Department of Meteorology, University of Maryland, College Park, Maryland 20742 (email: alan@atmos.umd.edu; gera@atmos.umd.edu)

K. E. Taylor, Lawrence Livermore National Laboratory, P.O. Box 808, Livermore, California 94550 (email: ktaylor@zooks.llnl.gov)

Y. Liu, Center for Analysis and Prediction of Storms, University of Oklahoma, Norman, Oklahoma 73019 (email: yuhe@tornado.gcn.uoknor.edu)

(Received February 14, 1995; revised June 29, 1995; accepted June 30, 1995)